Gas-Phase Fragmentation Reactions of Protonated Aromatic Amino Acids: Concomitant and Consecutive Neutral Eliminations and Radical Cation Formations

Houssain El Aribi, Galina Orlova, Alan C. Hopkinson, and K. W. Michael Siu*

Department of Chemistry and Centre for Research in Mass Spectrometry, York University, 4700 Keele Street, Toronto, Ontario, Canada M3J 1P3

Received: November 16, 2003; In Final Form: February 16, 2004

Gas-phase dissociation reactions of protonated amino acids—phenylalanine, tyrosine, tryptophan, and histidine—are rich and diverse. Considerable similarities exist among the four amino acids, but there are also significant differences. Facile reactions include the elimination of NH_3, common to all aromatic amino acids except histidine, and the concomitant elimination of H_2O and CO. Labeling experiments with deuteriums show considerable H/D scrambling prior to dissociation involving N−H, O−H, and C−H (both aliphatic and aromatic hydrogens). Mechanisms of this scrambling are proposed. At higher collision energies, eliminations of H_2O, CO, CO_2, and CH_2CO occur after that of NH_3. Similarly, eliminations of HCN, $HCNH_2$, and NH_3 occur after that of H_2O and CO. The elimination of CH_2CO is preceded by migration of the hydroxyl ion from the carboxylic group to the exocyclic carbon on the side chain. Aromatic amino acids, with the exception of tyrosine, were observed to yield cationic radical fragments by eliminating small radicals, including $H^{\bullet}$, $CH_3^{\bullet}$, and $NH{=}CH^{\bullet}$.

Introduction

The dissociation reactions of protonated amino acids (AAs) have attracted considerable attention, in part because they may serve as models for the fragmentation of protonated peptides in gas-phase microsequencing using tandem mass spectrometry. A variety of ionization techniques have been utilized in these studies, including electron impact,[1−3] chemical ionization,[4−12] field desorption,[13] secondary ion mass spectrometry,[14−16] fast atom bombardment,[17−19] laser ionization,[20−24] atmospheric pressure ionization,[25] plasma desorption,[26] and electrospray ionization.[27,28] Quantum chemistry methods have also been used to investigate some of these reactions;[28−32] however, few fragmentation mechanisms have been examined in detail. Studies on the dissociations of protonated AAs have tended to concentrate on AAs that bear alkyl side chains, mainly because they produce simpler collision-induced dissociation (CID) spectra and their small size permits the use of high-level first principle methods to obtain accurate structures and energetics. It has been shown that protonated aliphatic AAs fragment predominantly to form their respective iminium ions by concomitant loss of H_2O and CO, giving rise to very simple CID mass spectra. Hydroxylic and acidic AAs, those with OH and COOH groups in their side chains, show aside from the loss of (H_2O + CO) an additional loss of H_2O from the side chain. Amidic AAs, those with an amide group in the side chain, and aromatic AAs exhibit an additional loss of NH_3.

Here, we report that the fragmentation chemistries of protonated aromatic AAs—phenylalanine, tyrosine, tryptophan, and histidine—are far richer and more complicated than have previously been recognized. This study represents, therefore, the first detailed examination of the gas-phase fragmentation chemistries of protonated aromatic AAs. The aromatic AAs were ionized using electrospray; the protonated ions were collisionally activated under laboratory energies of tens of eV, and their fragmentation products were mass-analyzed using a downstream quadrupole. Abundant fragment ions were observed and are identified; detailed fragmentation schemes are proposed. While similarities do exist in the dissociation chemistries of the four protonated aromatic AAs, it will be shown that that there are also some significant differences. Some of the unique chemistries will be highlighted.

Experimental Section

Experiments were conducted on MDS Sciex (Concord, ON) API III and API 3000-prototype triple-quadrupole mass spectrometers. Energy-resolved CID experiments were performed only on the API III mass spectrometer under single-collision conditions. The aromatic AAs (99% purity) used in this study were commercially available from Aldrich Chemical Corporation (St. Louis, MO). All solvents used were high-performance liquid chromatography (HPLC) grade and were also from Aldrich Chemical Corporation. Sample solutions were 10 μM of aromatic AA in 30/70 H_2O/CH_3OH. When needed, H/D exchange experiments were carried out by dissolving the aromatic AA in deuterium oxide (99.9 atom % in D, Aldrich) and CH_3OD (99.5 atom % in D, Aldrich), instead of H_2O and CH_3OH. The sample solution was introduced into the pneumatically assisted electrospray source using a syringe pump (Harvard Apparatus, Model 22, South Natick, MA) at a typical flow rate of 2 μL/min with dry air being the nebulizer gas. Mass analysis of the ions was performed at unit-mass resolution at a step size of 0.1 Th and at a dwell time of 50 ms/step. CID experiments were performed with argon (API III) and nitrogen (API 3000) as the neutral collision gas partner. The protonated AA was mass-selected with the first quadrupole, Q1, and accelerated to a known kinetic energy defined by the charge of the ion (+1) and the potential difference between the quadupolar lens, q0, upstream from Q1 and the second quadrupole, q2. The fragment ions produced in q2 were mass-analyzed using the third quadrupole, Q3. Energy-resolved CID was performed by varying

* Address correspondence to this author. Tel: (416) 650-8021; fax: (416) 736-5936; e-mail: kwmsiu@yorku.ca.

10.1021/jp0374915 CCC: $27.50
Published on Web 04/03/2004

TABLE 1: CID of Protonated Aromatic AAs at E_{lab} = 30 V: *m/z* Ratios, H/D Exchange Shifts in Italics, and Relative Ion Abundances in Parentheses

amino acid	precursor ion	more abundant fragments (≥25%)		less abundant fragments (<25%)			radicals
Phe	166 + *4*	120 + *2−3* (100%)	103 + *1−2* (25%)	107 + *1−2* (8%) 118 + *1* (6%) 149 + *1−2* (4%)	77 + *1* (7%) 91 + *1−2* (4%) 93 + *2−3* (4%)	79 + *1−2* (6%) 131 + *1* (5%)	119 + *1−2* (23%)
Tyr	182 + *5*	136 + *3−4* (100%) 123 + *2−3* (45%)	91 + *1−2* (52%) 119 + *1−3* (26%)	165 + *2−3* (19%) 147 + *1−2* (7%) 103 + *1* (5%)	95 + *2−3* (17%) 77 + *1−2* (7%) 65 + *1−2* (5%)	107 + *1−3* (12%) 121 + *1−2* (5%) 53 + *2* (4%)	
Trp	205 + *5*	146 + *2−4* (100%) 144 + *2−4* (40%)	118 + *2−4* (75%) 132 + *2−4* (38%)	188 + *2−4* (23%) 142 + *2−3* (19%) 74 + *2* (7%)	170 + *1−3* (20%) 130 + *2−3* (19%)	159 + *3−4* (20%) 91 + *2* (10%)	143 + *1−2* (28%) 117 + *1−2* (25%) 115 + *1−2* (17%)
His	156 + *5*	83 + *2−3* (100%) 93 + *1−3* (67%) 56 + *1−3* (28%)	110 + *3−4* (88%) 95 + *2−3* (31%)	81 + *1−2* (22%) 42 + *1* (3%)	68 + *1−3* (24%)	66 + *1* (10%)	82 + 2 (44%)

the center-of-mass energy of the protonated AA and measuring the abundances of the product ions. Investigations of ion lineage sometimes required additional stages of tandem mass spectrometry; pseudo-MS^3 experiments were performed by raising the orifice bias voltage to generate in the lens region the desired fragment ion, which was then mass-selected with Q1, fragmented in q2, and its next-generation product ions mass-analyzed in Q3. Precursor ions of a particular fragment ion were located by precursor ion scans, in which Q1 was scanned and Q3 set to transmit only the fragment ion of interest.

Calculations

The structures and energetics of selected ions were calculated with density functional theory (DFT) using the hybrid B3LYP exchange correlation functional[33−35] with the 6-31+G* doubly split-valence basis set[36−39] in Gaussian 98.[40] All stationary points were characterized by harmonic vibrational frequency calculations. The connections between transition-state structure and minima on the potential energy surface were established using the intrinsic reaction coordinates technique as implemented in Gaussian 98.[40]

Results and Discussion

Electrospraying a solution of 10 μM aromatic AA in 30/70 H_2O/CH_3OH produces abundant protonated aromatic amino acid ions. For Phe, Tyr, and Trp, the most probable protonation site is on the nitrogen atom of the α-amino group, whereas for His, it is on the imino nitrogen in the imidazole ring.[41] The dissociations of protonated aromatic AA (Figures 1−4, E_{lab} = 30 V) show a variety of common fragmentation pathways, including the concomitant loss of (H_2O + CO), and subsequently HCN, CH_2NH, and NH_3; the elimination of NH_3, and subsequently H_2O, CO, CO_2, and CH_2CO; and the formation of radical cationic products. Protonated His is an exception in that eliminations of NH_3, and the sum of NH_3 and H_2O, are not observed, probably because protonation occurs on the imidazole ring as opposed to on the α-amino nitrogen. However, the concomitant loss of (NH_3 + CO_2) and the elimination of NH_3 after the loss of (H_2O + CO) do occur. At relatively high collision energies (E_{lab} > 20 V), protonated Phe and His fragment to yield a minimum of one and protonated Trp three radical cationic products. Under these conditions, protonated Tyr does not yield any radical ions. Table 1 summarizes the fragment ions observed and Tables 2−5 list the most probable neutral losses that lead to the observed fragment ions. In the neutral losses involving deuterium-containing AAs, multiple possibilities exist regarding deuterium incorporation in some of the neutral fragments. For brevity, not all possible combinations are listed. In addition, some low abundant ions are not listed because they may be formed via several competitive pathways involving different neutral losses.

Loss of NH_3 and Beyond. Elimination of NH_3 is observed from protonated Phe, Tyr, and Trp but not from protonated His. Energy-resolved CID experiments demonstrated that for protonated Tyr and Trp, this fragmentation channel has the lowest energy threshold, whereas for protonated Phe, only the concomitant loss of (H_2O + CO) is lower in threshold (Figures 1−3). Harrison's group[42] has proposed a mechanism for the loss of NH_3 from protonated Tyr in which the phenolic group migrates to form the phenonium ion with concomitant elimination of NH_3. This same mechanism was also invoked by Rogalewicz et al.[27] who emphasized the electron-donating property of the phenolic OH in stabilizing the phenonium ion. Both Rogalewicz's and our results support this interpretation; the loss of NH_3 is approximately 5 times more abundant in protonated Tyr than in protonated Phe (Table 1 and Figures 1 and 2). As pointed out by Shoeib et al.,[43] an alternative mechanism for the elimination of NH_3 involves a benzyl cation. Thermodynamically, the benzyl cation is lower in free energy than the phenonium ion by 14.1 kcal/mol at the B3LYP/6-31++G(d,p) level of theory; however, the 1,2-hydride shift that precedes formation of the former has a free-energy barrier of 36.5 kcal/mol, while formation of the latter is simply the endoergicity of the reaction. A similar, bridged structure in which the positive charge is located on the nitrogen atom in the imidazole ring can be drawn for the ion formed by the loss of NH_3 from protonated tryptophan.

TABLE 2: Neutral Fragments Lost in CID of Protonated Phenylalanine and deuteronated d_3-Phenylalanine at E_{lab} = 20 V[a]

protonated phenylalanine (m/z = 166)		deuteronated d_3-phenylalanine (m/z = 170)		
fragment ions (m/z)	neutrals lost	fragment ions (m/z)	neutrals lost	competitive loss ratio
149	NH_3	150, 151	ND_3, ND_2H	2:1
131	($NH_3 + H_2O$)	131, 132	(ND_3 + HDO), (ND_2H + HDO)	1:2
120	(H_2O + CO)	122, 123	(D_2O + CO), (HDO + CO)	5:1
107	($NH_3 + CH_2CO$)	108, 109	($ND_3 + CH_2CO$), ($ND_2H + CH_2CO$)	3:1
105	($NH_3 + CO_2$)	105, 106	($ND_3 + CO_2$), ($ND_2H + CO_2$)	1:2
103	($NH_3 + H_2O$ + CO)	103, 104, 105	(ND_3 + HDO + CO), (ND_2H + HDO +CO), (NH_2D + HDO +CO)	1:3:2
93	(H_2O + CO + HCN)	95, 96	(D_2O + CO + HCN), (HDO + CO + HCN)	4:1
91	(H_2O + CO + HCN + H_2)	92, 93	(D_2O + CO + HCN + HD), (D_2O + CO + HCN + H_2)	1:1
79	($NH_3 + CH_2CO$ + CO)	80, 81	($ND_3 + CH_2CO$ + CO), ($ND_2H + CH_2CO$ + CO)	4:1
77	($NH_3 + CH_2CO$ + CO + H_2)	78, 79	($ND_3 + CH_2CO$ + CO + H_2), ($ND_2H + CH_2CO$ + CO + H_2)	2:1

[a] Some ions, e.g., 119 and 118 Th, are not listed because competitive loss ratios were ambiguous.

TABLE 3: Neutral Fragments Lost in CID of Protonated Tyrosine and Deuteronated d_4-Tyrosine at E_{lab} = 20 V

protonated tyrosine (m/z = 182)		deuteronated d_4-tyrosine (m/z = 187)		
fragment ions (m/z)	neutrals lost	fragment ions (m/z)	neutrals lost	competitive loss ratio
165	NH_3	167, 168	ND_3, ND_2H	3:1
147	($NH_3 + H_2O$)	148, 149	(ND_3 + HDO), (ND_2H + HDO)	1:2
136	(H_2O + CO)	139, 140	(D_2O + CO), (HDO + CO)	6:1
123	($NH_3 + CH_2CO$)	125, 126	($ND_3 + CH_2CO$), ($ND_2H + CH_2CO$)	4:1
121	($NH_3 + CO_2$)	121, 122	($ND_3 + CO_2$), ($ND_2H + CO_2$)	1:1
119	($NH_3 + H_2O$ + CO)	120, 121, 122	(ND_3 + HDO + CO) (ND_2H + HDO + CO), (NH_2D + HDO + CO)	1:2:1
107	(H_2O + CO + CH_2NH)	108, 109, 110	(D_2O + CO + CH_2ND), (HDO + CO + CH_2ND), (HDO + CO + CH_2NH)	1:2:1
103	($NH_3 + H_2O + CO_2$)	104	($ND_2H + D_2O + CO_2$)	
95	($NH_3 + CO_2 + C_2H_2$)	97, 98	($ND_3 + CO_2 + C_2H_2$), ($ND_2H + CO_2 + C_2H_2$)	1:6
91	(H_2O + CO + NH_3 +CO)	92, 93, 94	(D_2O + CO + ND_2H + CO), (HDO + CO + ND_2H + CO), (HDO + CO + NH_2D + CO)	1:2:1
77	($NH_3 + CO_2 + C_2H_2 + H_2O$)	78, 79	($ND_3 + CO_2 + C_2H_2$ + HDO), ($ND_2H + CO_2 + C_2H_2$ + HDO)	5:1

The dissociations of deuteronated (addition of a deuteron) d_3-Phe, d_4-Tyr, and d_4-Trp are informative. These ions have formally had their N−H and O−H hydrogens exchanged for deuteriums and, in addition, have the ionizing deuteron. The results (Tables 2−5) show, however, competitive losses of ND_3 and ND_2H in a ratio of 2:1 and 3:1 from, respectively, deuteronated d_3-Phe and d_4-Tyr and competitive losses of ND_3, ND_2H, and NDH_2 in ratios of 1:2:1 from deuteronated d_4-Trp. These results indicate considerable H/D scrambling between N−D/O−D and C−H prior to ammonia elimination. Rogalewicz et al.[27] reported also the loss of partially deuterated ammonia for deuterated Trp, but only ND_3 for deuterated Tyr. A question that arose from the scrambling was which hydrogens, the aliphatic or aromatic C−H hydrogens, are involved? To answer this question, we performed CID experiments on protonated phenyl-d_5-alanine that contains five deuteriums on its phenyl ring and deuteronated d_8-[phenyl-d_5-alanine] (i.e., deuterated Phe that contains eight incorporated deuteriums). The results (E_{lab} = 15 V) are summarized in Table 6. The fragmentation of protonated phenyl-d_5-alanine shows competitive losses of NH_3 and NH_2D in a ratio of 3:1, thereby supporting H/D scrambling and indicating participation of the deuteriums from the phenyl ring in the scrambling reactions. Deuteronated d_8-[phenyl-d_5-alanine] also shows competitive losses of ND_3 and NHD_2 in a ratio of 3:1, indicating participation of the aliphatic hydrogen atoms in H/D scrambling. These results thus signify (probably extensive) scrambling of N−H/O−H, aliphatic C−H, and aromatic C−H hydrogens prior to ammonia elimination.

Proposed mechanisms of the scrambling reactions are shown in Figure 5. Structure **I** is the lowest energy isomer of protonated Phe. Bond rotations lead to rotamer **II** that is 9.2 kcal/mol higher in free energy at 298 K. A double proton transfer then occurs from the protonated amino group to the carbonyl oxygen and from the hydroxyl group to the δ-carbon to yield structure **III**. The reverse process is virtually barrierless: the difference in energy between **III** and **II** (19.9 kcal/mol in free energy) is primarily due to the loss of aromaticity in the ring. Ion **II** can be re-formed from **III**, and in the process a different proton on the δ-carbon can be transferred to oxygen (details not shown). This will result in H/D scrambling in deuteronated d_3-Phe. A very recent article that appeared after submission of the first version of this report rationalizes H/D scrambling in deuter-

TABLE 4: Neutral Fragments Loss in CID of Protonated Tryptophan and Deuteronated d_4-Tryptophan at E_{lab} = 20 V[a]

protonated tryptophan (m/z = 205)		deuteronated d_4-tryptophan (m/z = 210)		
fragment ions (m/z)	neutrals lost	fragment ions (m/z)	neutrals lost	competitive loss ratio
188	NH_3	190, 191, 192	ND_3, ND_2H, NDH_2	1:2:1
170	(NH_3 + H_2O)	171, 172, 173	(ND_3 + HDO), (ND_2H + HDO), (ND_2H + HDO)	1:2:1
159	(H_2O + CO)	162, 163	(D_2O + CO), (HDO + CO)	1:1
146	(NH_3 + CH_2CO)	148, 149, 150	(ND_3 + CH_2CO), (ND_2H + CH_2CO), (ND_2H + CH_2CO)	2:4:1
144	(NH_3 + CO_2)	146, 147, 148	(ND_3 + CO_2), (ND_2H + CO_2), (NDH_2 + CO_2)	1:1:1
143	(NH_3 + CO_2 + H•)	143, 144	(ND_3 + CO_2 + D•), (ND_3 + CO_2 + H•) or (ND_2H + CO_2 + D•)	1:1
142	(NH_3 + H_2O + CO)	143, 144, 145	(ND_3 + HDO + CO), (ND_2H + HDO + CO), (NH_2D + HDO + CO)	1:2:1
132	(H_2O + CO + HCN)	134, 135, 136	(D_2O + CO + DCN), (D_2O + CO + HCN), (HDO + CO + HCN)	1:3:3
130	(H_2O + CO + HCN + H_2)	132, 133	(D_2O + CO + HCN + HD), (D_2O + CO + HCN + H_2)	1:1
118	(NH_3 + CH_2CO + CO)	120, 121, 122	(ND_3 + CH_2CO + CO), (ND_2H + CH_2CO + CO), (NDH_2 + CH_2CO + CO)	2:4:1

[a] Some ions, e.g., 117 and 115 Th, are not listed because competitive loss ratios were ambiguous.

TABLE 5: Neutral Fragments Lost in CID of Protonated Histidine and Deuteronated d_4-Histidine at E_{lab} = 20 V

protonated histidine (m/z = 156)		deuteronated d_4-histidine (m/z = 161)		
fragment ions (m/z)	neutrals lost	fragment ions (m/z)	neutrals lost	competitive loss ratio
110	(H_2O + CO)	113, 114	(D_2O + CO), (HDO + CO)	3:1
95	(NH_3 + CO_2)	97, 98	(ND_3 + CO_2), (ND_2H + CO_2)	2:1
93	(H_2O + CO + NH_3)	93,94,95,96	(D_2O + CO + ND_3), (D_2O + CO + ND_2H), (HDO + CO + ND_2H), (HDO + CO + ND_2H)	1:5:10:4
83	(H_2O + CO + HCN)	85, 86, 87	(D_2O + CO + DCN), (D_2O + CO + HCN), (HDO + CO + HCN)	5:5:1
82	(H_2O + CO + HCN + H•)	84	(D_2O + CO + DCN + H•), or (D_2O + CO + HCN + D•),	
81	(H_2O + CO + CH_2NH)	82, 83	(D_2O + CO + HDC═ND), (D_2O + CO + H_2C═ND),	1:4
68	(NH_3 + CO_2 + HCN)	70, 71	(ND_3 + CO_2 + HCN), (ND_2H + CO_2 + HCN)	1:2
66	(H_2O + CO + NH_3 + HCN)	67, 68, 69	(D_2O + CO + ND_2H + HCN), (HDO + CO + ND_2H + HCN) (HDO + CO + NDH_2 + HCN)	1:2:3
56	(H_2O + CO + HCN + HCN)	57, 58, 59	(D_2O + CO + DCN + DCN), (D_2O + CO + HCN + DCN), (D_2O + CO + HCN + HCN)	1:4:3

onated d_4-Trp via proton transfer between the protonated amino group and C2 of the indole.[44] Attempts to find an equivalent mechanism in deuteronated d_3-Phe were unsuccessful as the transferred proton immediately jumped back from the δ-carbon (C2) to the amino nitrogen. Scrambling involving the methylene hydrogens can now take place via ion **III**. Again, a double proton transfer from the methylene carbon to the carbonyl oxygen and from the hydroxyl group to the amino nitrogen via **TS(III→IV)** takes place to form ion **IV**. The free-energy barrier for this step is 24.4 kcal/mol. Direct transfer of the methylene proton of **III** to the amino nitrogen can also occur via **TS(III→IV)′**; this pathway exhibits a larger free-energy barrier of 28.6 kcal/mol. Protonated Phe is likely to be electrosprayed into the gas phase solvated by methanol and water molecules. Scrambling of N−H/O−H, aliphatic C−H, and aromatic C−H hydrogens can take place in the free jet downstream from the orifice and in the vicinity of the quadrupolar lens (q0). In these regions, many collisions with nitrogen, water, and methanol molecules take place. A solvating water or methanol molecule can catalyze proton transfer or participate in proton switching.[45] This is illustrated in Figure 5 in the proton switching reaction that involves a methylene hydrogen in the methanol-solvated ion **V**, which is a solvated rotamer of **III**. The free-energy barrier of the proton switching reaction via **TS(V→VI)** is relatively low (14.4 kcal/mol). The product ion **VI** is a methanol-solvated rotamer of ion **IV**.

As reported earlier, protonated His does not appear to eliminate NH_3. This is consistent with the results of the Harrison group[42] and Rogalewicz et al.,[27] but in contrast to those of Kulik et al.[20] who reported the loss of NH_3. We attribute the absence of this channel in protonated His to protonation of the imino nitrogen on the imidazole ring, as opposed to the α-amino nitrogen in the other aromatic AAs.

Results of the energy-resolved CID experiments (Figures 1−3) clearly show that the product ion formed via elimination of NH_3 (the aforementioned phenonium ion) will further

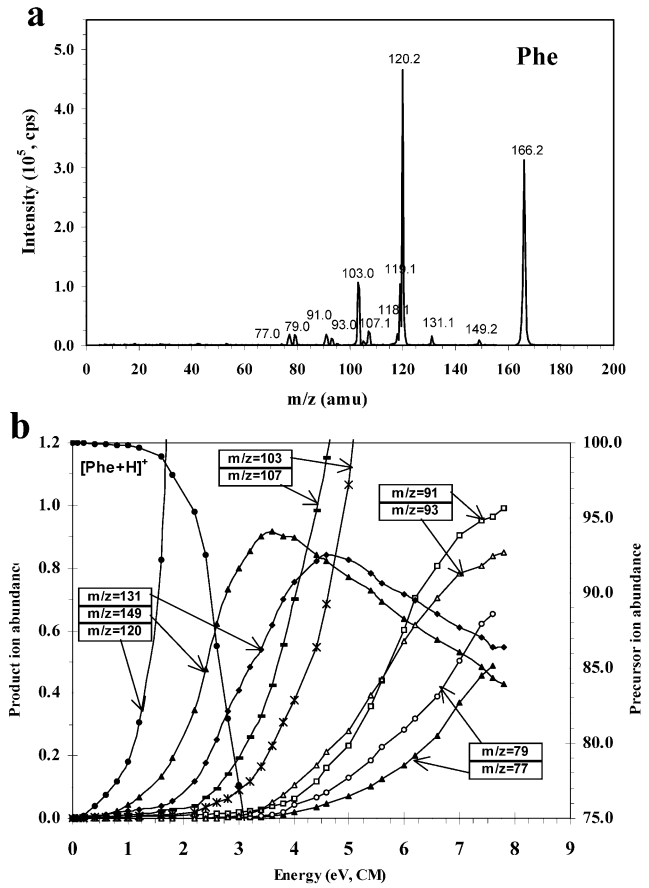

Figure 1. (a) CID spectrum of protonated phenylalanine obtained on the API 3000 under multiple-collision conditions with N_2 at $E_{lab} = 30$ V; (b) energy-resolved CID of protonated phenylalanine obtained on the API III under single-collision conditions with Ar.

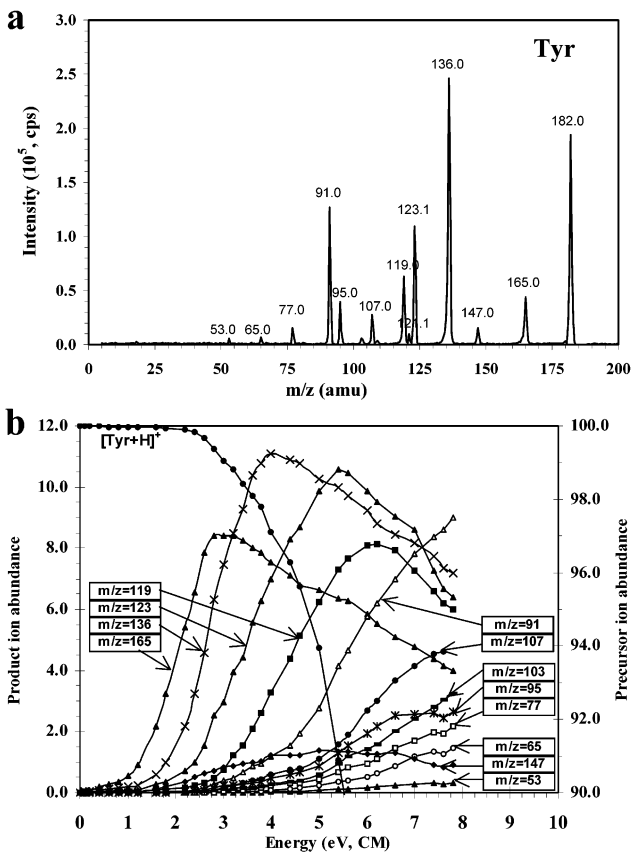

Figure 2. (a) CID spectrum of protonated tyrosine obtained on the API 3000 under multiple-collision conditions with N_2 at $E_{lab} = 30$ V; (b) energy-resolved CID of protonated tyrosine obtained on the API III under single-collision conditions with Ar.

fragment under relatively high-energy collisions ($E_{cm} > 2.5$ eV). The phenonium ion and its tautomers are carbocations[46] that have limited stability in the gas phase.[47−51] Scheme 1 shows proposed mechanisms for some of the observed fragmentation reactions. The ion lineages were established by product as well as precursor ion scans. The losses of H_2O followed by CO (Scheme 1, pathway A) from the phenonium ion, structure **VII**, are observed in significant abundances. Elimination of H_2O yields ion **X**, a benzyl cation with a ketene attached to the cationic carbon. The acylium ion, R′−CH═CH−C^+═O, is a resonance structure of ion **X**. This ion can lose CO facilely, in accordance with experimental results at $E_{cm} > 4.5$ eV (Figures 1−3). This channel is absent in protonated His. The product formed after CO loss is a vinyl cation stabilized by an electron-donating group on the cationic carbon. Product ions of identical *m*/*z* values for protonated Phe undergoing metastable decomposition have been reported.[42] There were, however, no comments on their possible identities.

The loss of CO_2 from ion **VII**, (Scheme 1, pathway B), is also observed, but the product ion abundance is low for protonated Phe and Tyr, relative to that for protonated Trp. The phenonium ion, **VII**, opens up (Scheme 1, pathway B); a 1,2-hydride shift then ensues to give the R′−C^+H−CH_2–COOH ion. Elimination of CO_2 yields ion **IX**. Interestingly, ion **IX** (and/or an isomer of it) is a prominent fragment for protonated His, although the latter does not lose NH_3 independently. A product ion having the *m*/*z* value corresponding to the loss of NH_3 and CO_2 was also observed in the metastable decomposition of protonated His.[42] The ion derived from histidine then loses HCN facilely to form probably an acyclic ion (vide infra). For protonated Trp and His, ion **IX** further fragments under high collision energies to yield radical cationic fragments (vide infra).

An interesting common channel is formation of the R′$CHOH^+$ fragment (Scheme 1, pathway C), which may result from migration of the hydroxide ion from the carboxylic group to the carbon adjacent to the ring followed by elimination of ketene, CH_2CO, to form a protonated aromatic aldehyde. A reaction profile for phenylalanine ions is shown in Figure 6. The migration of the hydroxide ion in ion **XI** is probably facilitated by the charge on the benzylic carbon, which should also reduce the barrier to eliminating ketene. The hydroxide ion migration step has a barrier of 25.1 kcal/mol, in terms of free energy at 298 K. The elimination of ketene has a cumulative free-energy barrier of 25.6 kcal/mol. Migration of the methoxy ion has been proposed in the dissociation of protonated methyl cinnamate that leads to ketene elimination.[52]

Concomitant Loss of (H_2O + CO): Formation of Iminium Ion and Beyond. Formation of the iminium ion (loss of 46 Da) was observed from all protonated aromatic AAs; it is typically the most prominent fragmentation channel at relatively low collision energies. The exception to this generalization is protonated Trp, where the intensity is only 15% and the loss of NH_3 is the most prominent channel at $E_{cm} < 2.5$ eV. Observation of this small but significant channel is in accordance with earlier reports.[20,24,26,42] Rogalewicz et al.,[27] however, explicitly reported absence of the iminium ion and rationalized it by invoking the relatively high proton affinity (PA) of Trp (PA = 227 kcal/mol[53] and 220.7 kcal/mol[41]), which they took as a manifestation

TABLE 6: Neutral Fragments Lost in CID of Protonated and Deuteronated d_8-Phenyl-d_5-alanine at E_{lab} = 20 V

protonated phenyl-d_5-alanine (m/z = 171)			deuteronated d_8-phenyl-d_5-alanine (m/z = 175)		
fragment ions (m/z)	neutrals lost	competitive loss ratio	fragment ions (m/z)	neutrals lost	competitive loss ratio
154, 153	NH_3, NH_2D	3:1	156, 155	ND_2H, ND_3	1:3
136, 135, 134	($NH_3 + H_2O$); ($NDH_2 + H_2O$)or(NH_3 + HDO); ($ND_2H + H_2O$), (NDH_2 + HDO) or ($NH_3 + D_2O$)	1:2:1	137, 136, 135	(ND_2H + HDO), ($NDH_2 + D_2O$) or ($ND_3 + H_2O$); ($ND_2H + D_2O$) or (ND_3 + HDO); ($ND_3 + D_2O$)	1:2:1
125, 124	(H_2O + CO), (HDO + CO)	5:1	125, 124	(D_2O + CO), (HDO + CO)	5:1

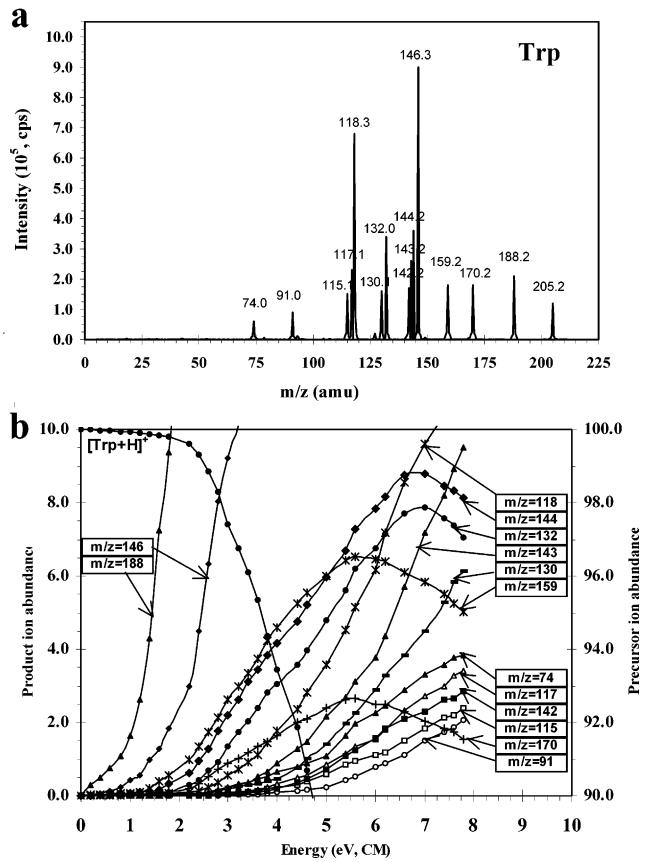

Figure 3. (a) CID spectrum of protonated tryptophan obtained on the API 3000 under multiple-collision conditions with N_2 at E_{lab} = 30 V; (b) energy-resolved CID of protonated tryptophan obtained on the API III under single-collision conditions with Ar.

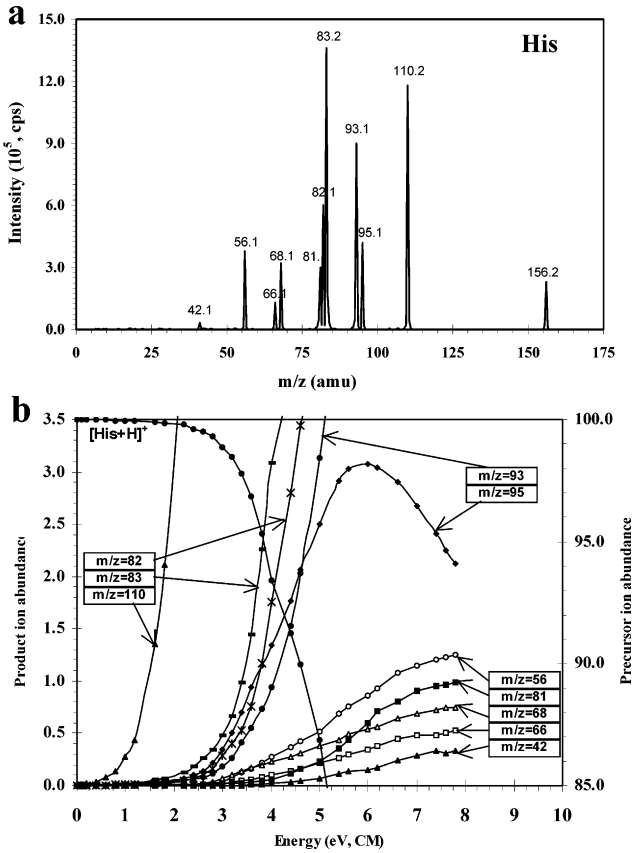

Figure 4. (a) CID spectrum of protonated histidine obtained on the API 3000 under multiple-collision conditions with N_2 at E_{lab} = 30 V; (b) energy-resolved CID of protonated histidine obtained on the API III under single-collision conditions with Ar.

of side chain protonation. This expectation is in disagreement with the computational studies of Maksić and Kovačević,[41] who reported protonation on the α-amino nitrogen for Phe, Tyr, and Trp; the only aromatic AA that protonates on the side chain is His.

The mechanism of the 46 Da loss presumably does not depend on the side chain of the amino acid. Several reaction mechanisms regarding the neutral loss of 46 Da from protonated AAs have been proposed.[5−13] There have also been experimental attempts to identify the structure of the 46 Da neutral using collision-induced dissociative ionization[20] and neutralization−reionization.[54] Neither of these two studies provided sufficient evidence to establish that the neutral loss of 46 Da occurred as a single molecule, formic acid. Alternative candidates that have been proposed for this loss in protonated Gly include ($CO_2 + H_2$) and :$C(OH)_2$.[29,31,54] It is now believed that the loss of 46 Da is most probably due to the concomitant loss of H_2O and CO, which is kinetically more favorable than all other alternatives.[29,31,51,55] The concomitant loss of (H_2O + CO) has been reported to have a calculated activation barrier of 36.6 kca/mol[31] and 35.6 kcal/mol (the second as $H^{\ddagger}_{298}$ at QCISD(T)/6-31+G(d,p)).[29] These values are in accordance with our measured threshold energy of 38 kcal/mol (unpublished data; expected error ∼ ±3 kcal/mol[56−59]).

Scheme 1, pathway E, summarizes the concomitant elimination of H_2O and CO to form the iminium ion **VIII**.[29,31] It begins with a proton transfer from the $-NH_3^+$ group to the hydroxyl of the carboxylic group, followed by elimination of H_2O to form a transient acylium ion, which eliminates CO spontaneously to form the iminium ion.[29] No transient ion formed by elimination of water has ever been reported; furthermore, this ion was not detected in our study despite extensive experimentation. For protonated His, a proton transfer from the protonated nitrogen in the imidazole ring to the hydroxyl of the carboxylic acid is required prior to elimination of H_2O. This can take place either directly or indirectly via the α-amino group to which the imino proton is hydrogen-bonded in the structure at the global minimum. That formation of the iminium ion is energetically

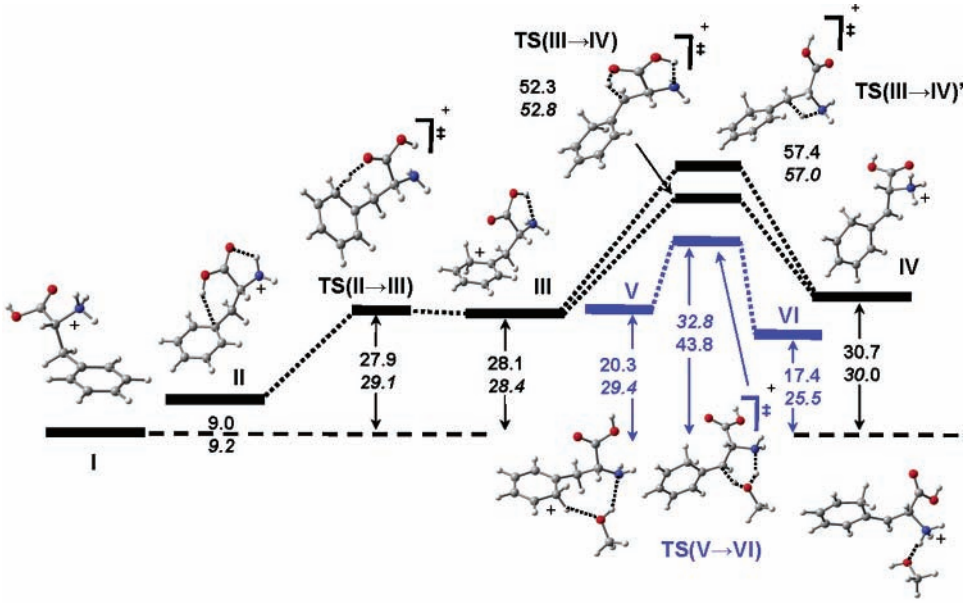

Figure 5. Intramolecular hydrogen transfer in protonated phenylalanine (profile in black) and methanol-solvated protonated phenylalanine (profile in blue) calculated at B3LYP/6-31+G*: upper number, $\Delta H_0°$; lower number in italics, $\Delta G_{298}°$ in kcal/mol. On the lower profile, energies are relative to **I** plus methanol at infinite separation. Gray, carbon; white, hydrogen; blue, nitrogen; and red, oxygen.

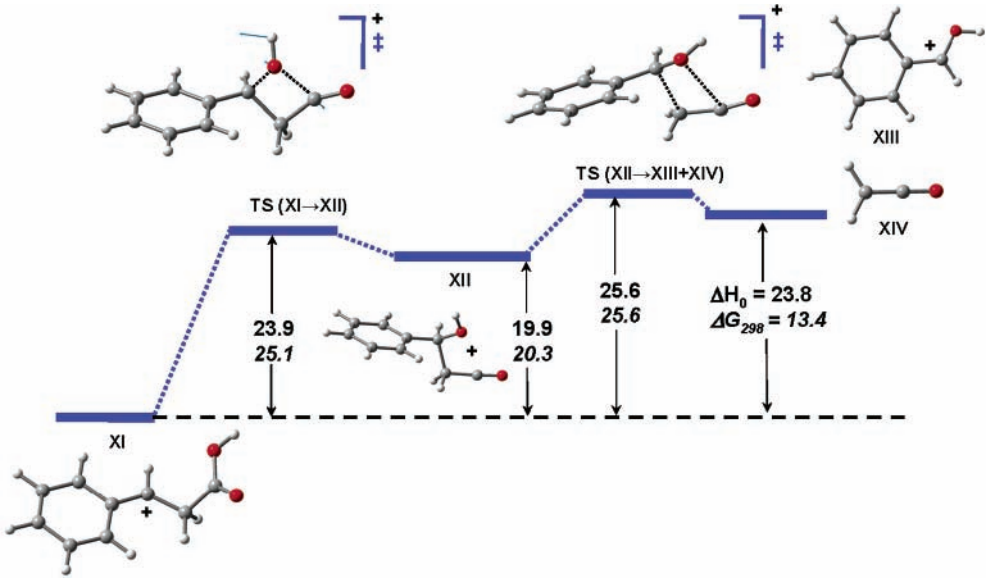

Figure 6. Reaction profile for OH migration and ketene elimination, after the loss of ammonia, in protonated phenylalanine calculated at B3LYP/6-31+G*: upper number, $\Delta H_0°$; lower number in italics, $\Delta G_{298}°$ in kcal/mol. Gray, carbon; white, hydrogen; and red, oxygen.

favorable is confirmed by energy-resolved CID experiments: it exhibits the lowest critical energy in protonated Phe (Figure 1) and protonated His (Figure 4), the second lowest in protonated Tyr (Figure 2), and the third lowest in protonated Trp (Figure 3).

As before, dissociations of deuterated aromatic AAs reveal H/D scrambling prior to formation of the iminium ions (Tables 2−5). Eliminations of (D_2O + CO) and (HDO + CO) were observed for all four aromatic AAs (Tables 2−5), in contrast to an earlier report.[27] Results for the dissociations of protonated phenyl-d_5-alanine and deuteronated d_8-[phenyl-d_5-alanine] are shown in Table 6. As before, eliminations of both H- and D-containing neutrals are strong indications of scrambling of N−H, O−H, aliphatic C−H, and aromatic C−H hydrogens (and deuteriums) prior to fragmentation. These observations support the findings of a recent report[60] on intramolecular H/D scrambling in deuterated peptides and their fragments. The exercise of caution is advised when it comes to structural interpretation involving H/D-exchange rates of peptides.

At relatively high collision energies (E_{cm} > 4 eV), the iminium ions **VIII** undergo further fragmentation (Scheme 1). The fragment ions that result from eliminations of NH_3, $HCNH_2$, and HCN are abundant for all four aromatic AAs (the exception is protonated Tyr for which the elimination of HCN is weak). Ion lineages were confirmed using precursor ion scans. The loss of NH_3 leads to prominent fragment ions, $R'-C^+=CH_2$, α-substituted vinyl cations in all four protonated aromatic AAs. The formation of $R'CH_2^+$ from **VIII** probably takes place via two routes, directly by eliminating $HCNH_2$, and indirectly by eliminating first HCN and then H_2.

Formation of Radical Cationic Fragments. Dissociation of protonated aromatic AAs results in formation of radical cations that, as far as we know, have never been reported. The *m*/*z* values for these radical cations are 119 Th for protonated Phe;

SCHEME 1

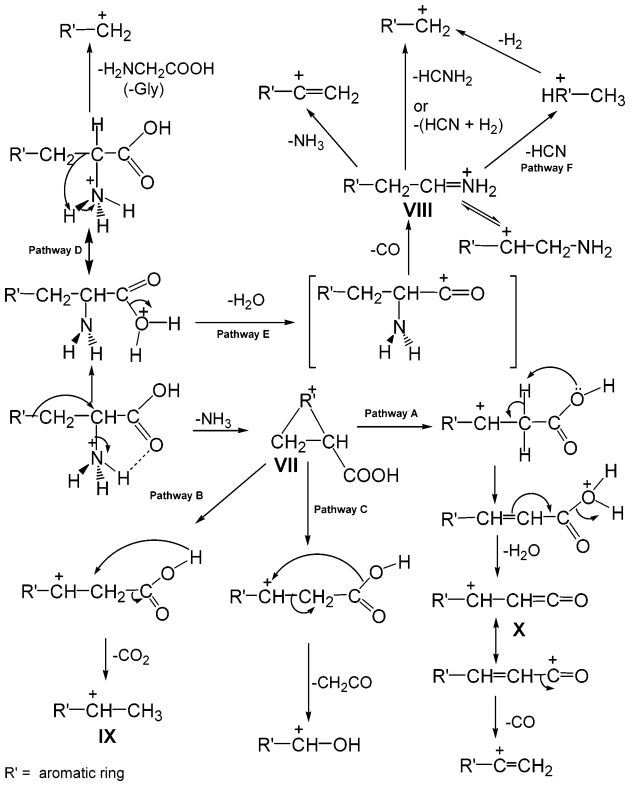

143, 117, and 115 Th for protonated Trp; and 82 Th for protonated His. No radical cation was observed in the fragmentation of protonated Tyr.

For Phe, precursor ion scans identified two precursors for the ion at 119 Th, the iminium ion, and protonated Phe (all precursor ion spectra are available as Supporting Information). The iminium ion at 120 Th is formed under very low collision energies (Figure 1) and is likely to be the intermediate from which elimination of H• occurs to give the radical cation at 119 Th, Ph−C•H−CH═NH_2^+. Scheme 2 shows proposed pathways for fragmentation of protonated Trp to give the three radical cations at 143, 117, and 115 Th. Precursor ion and CID experiments were used to determine ion lineage. Proposed structures are shown, guided by DFT calculations. Elimination of small radicals, H• and CH_3• from even-electron fragment ions results in radical cationic fragments. Scheme 3 shows a proposed pathway for protonated His. The radical that is eliminated to form the 82 Th ion is NH═CH•. The free-energy change at 298 K for this reaction is 65.9 kcal/mol, relatively high but in accordance with experimental conditions.

Formation of Other Ions. Scheme 3 also shows fragmentation pathways unique to protonated His in which elimination of HCN is involved. Concomitant elimination of H_2O and CO yields the ion **VIII** of His at 110 Th. This ion then fragments by eliminating NH═CH• to form the 82 Th ion, as discussed earlier, or by eliminating NH_3 to form an ion at 93 Th. The latter ion then opens up and eliminates HCN to give an acyclic ion at 66 Th. A formal structure with the positive charge on a carbon is given in Scheme 3, but in reality the charge is highly delocalized. A proposed reaction profile is given in Figure 7. The N_1-C_2 bond of the imidazole ring (structure **XV**) first cleaves. In one mechanism, the N_3-C_4 bond then cleaves to form $CH_2CCCHNH^+$ (ion **XXI**, 66 Th) and HCN. This reaction has a free-energy change of 67.8 kcal/mol at 298 K. Alternatively, fissure of the C_4-C_5 bond then ensues with concomitant transfer of the N_1-H hydrogen (a 1,5-hydride shift) to C_2 to

SCHEME 2

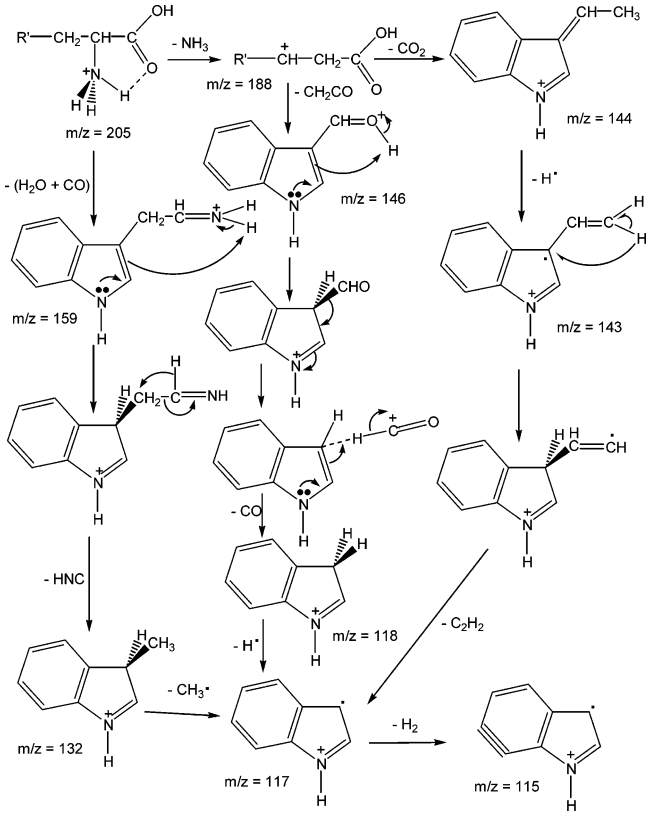

SCHEME 3

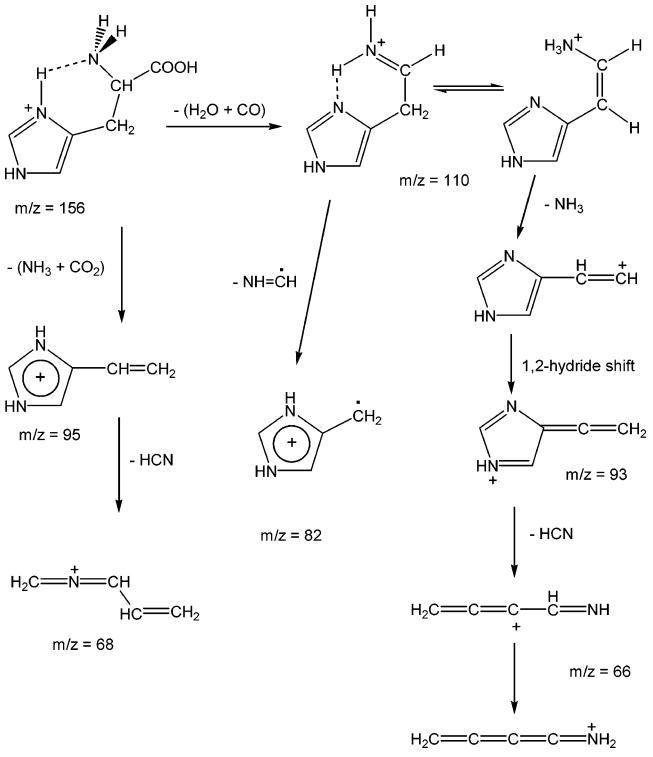

form $H_2CNCCCH_2^+$ (ion **XVII**, 66 Th) and HCN. This second reaction has a higher free-energy barrier of 75.7 kcal/mol. Experiments on $^{15}N_3$-histidine revealed loss of $HC^{15}N$ to $HC^{14}N$ in a ratio of 3 to 1, in accordance with the lower barrier for the loss of N_3 than that of N_1 in the elimination of HCN. A lower energy isomer of $CH_2CCCHNH^+$ is $CH_2CCCNH_2^+$ (Scheme 3). $CH_2CCCNH_2^+$ is 31.1 kcal/mol lower in free energy than

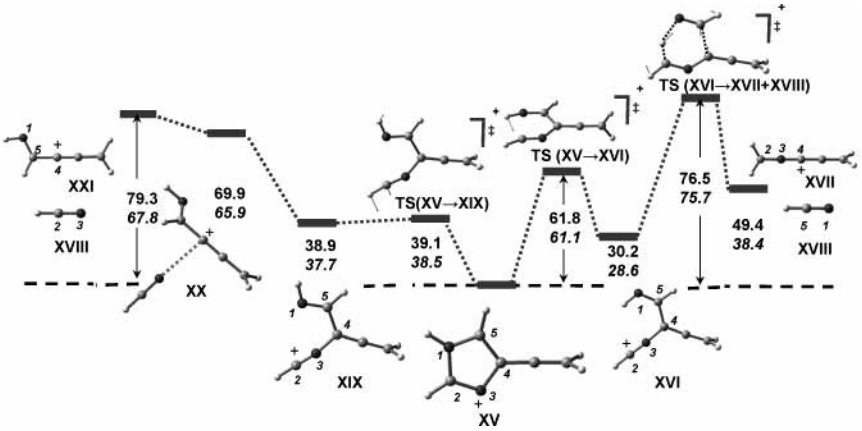

Figure 7. Reaction profile for HCN elimination from the 93 Th ion of protonated histidine calculated at B3LYP/6-31+G*: upper number, $\Delta H_0°$; lower number in italics, $\Delta G_{298}°$ in kcal/mol. Gray, carbon; white, hydrogen; and blue, nitrogen. Two mechanisms are shown for formation of the 66 Th ion. The one leading to $CH_2CCCHNH^+$ and HCN (shown in the left) has a lower free-energy barrier at 298 K.

$CH_2CCCHNH^+$; the barrier against converting the latter to the former via a 1,2-proton shift is 42.7 kcal/mol. A 95 Th ion, a tautomer of ion **IX** and similar in structure to the 93 Th ion discussed, is formed by concomitant elimination of NH_3 and CO_2. This 95 Th ion also loses HCN to give an acyclic, highly charge-delocalized ion at 68 Th. A proposed structure is shown in Scheme 3.

In addition, other unique but rather low abundance ions have also been observed in the dissociation of protonated aromatic AAs especially under relatively high-energy conditions, for example, the phenyl cation (77 Th) and the benzyl cation (91 Th) in Phe; the cyclopenta-1,3-dienyl cation (65 Th) and the cyclobutenyl cation (53 Th) in Tyr; protonated propionitrile, $CH_3-CH_2-C\equiv NH^+$ (56 Th) in His; and the ion $NH_2^+=CH-COOH$ (74 Th) in Trp.

Conclusions

This study has shown that, in addition to the concomitant loss of H_2O and CO (common in aliphatic AAs), aromatic AAs exhibit facile loss of NH_3. The only exception is histidine. Histidine protonates on the imidazole ring, instead of the N-terminal amino group, where the other three aromatic AAs protonate. Labeling experiments with deuteriums show considerable H/D scrambling prior to dissociation involving N−H, O−H, and C−H (both aliphatic and aromatic hydrogens). Eliminations of H_2O, CO, CO_2, and CH_2CO occur after that of NH_3, under higher collision energies. The loss of CH_2CO is preceded by migration of the hydroxyl ion from the carboxylic group to the exocyclic carbon on the side chain. Similarly, eliminations of HCN, $HCNH_2$, and NH_3 happen after the loss of H_2O and CO. In addition, aromatic AAs, except tyrosine, fragment to yield cationic radical fragments by eliminating small radicals, including $H^\bullet$, $CH_3^\bullet$, and $NH=CH^\bullet$.

Acknowledgment. We thank the Natural Sciences and Engineering Research Council of Canada (NSERC), MDS Sciex, the Canadian Foundation of Innovation (CFI), the Ontario Innovation Trust (OIT), and York University for supporting our work.

Supporting Information Available: Precursor ion scans of various fragment ions of protonated phenylalanine, tryptophan, and histidine, and Cartesian coordinates (Å) along with electronic energies (hartrees) for the structures examined. This material is available free of charge via the Internet at http://pubs.acs.org.

References and Notes

(1) Biemann, K.; McCloskey, J. A. *J. Am. Chem. Soc.* **1962**, *84*, 3192−3193.
(2) Junk, G.; Svec, H. *J. Am. Chem. Soc.* **1963**, *85*, 839−845.
(3) Heyns. K.; Grützmacher, H.-Fr. *Liebigs Ann. Chem.* **1963**, *667*, 194.
(4) Vetter, W. In *Biochemical Applications of Mass Spectrometry;* Waller, G. R., Ed.; Wiley: New York, 1972; p 387; 1980; Suppl. Vol. 1, p 439.
(5) Milne, G. W. A.; Axenrod, T.; Fales, H. M. *J. Am. Chem. Soc.* **1970**, *92*, 5170−5175.
(6) Meot-Ner, M.; Field, F. H. *J. Am. Chem. Soc.* **1973**, *95*, 7207−7211.
(7) Leclercq, P. A.; Desiderio, D. *Org. Mass Spectrom.* **1973**, *7*, 515−533.
(8) Tsang, C. W.; Harrison, A. G. *J. Am. Chem. Soc.* **1976**, *98*, 1301−1308.
(9) Hunt, D. F.; Shabanowitz, J.; Botz, F. K. *Anal. Chem.* **1977**, *49*, 1160−1163.
(10) Beuhler, R. J.; Flanigan, E. L.; Greene, L. J.; Friedman, L. *J. Am. Chem. Soc.* **1974**, *96*, 3990−3999.
(11) Volgt, D.; Schmidt, J. *Biomed. Mass Spectrom.* **1978**, *5*, 44−46.
(12) Vairamani, M.; Srinivas, R.; Viswanadha Rao, G. K. *Indian J. Chem., Sect. B* **1988**, *27*, 284−285.
(13) Eckersley, M.; Bowie, J. H.; Hayes, R. N. *Int. J. Mass Spectrom. Ion Processes* **1989**, *93*, 199−213.
(14) Winkler, H. U.; Beckey, H. D. *Org. Mass Spectrom.* **1972**, *6*, 855−860.
(15) Benninghoven, A.; Jaspers, D.; Sichtermann, W. *Appl. Phys.* **1976**, *11*, 35−39.
(16) Benninghoven, A.; Sichtermann, W. *Anal. Chem.* **1978**, *50*, 1180−1184.
(17) Liu, L. K.; Busch, K. L.; Cooks, R. G. *Anal. Chem.* **1981**, *53*, 109−113.
(18) Zwinselman, J. J.; Nibbering, N. M. M.; Van der Greef, J.; Ten Noever de Brauw, M. C. *Org. Mass Spectrom.* **1983**, *18*, 525−529.
(19) Van der Greef, J.; Ten Noever de Brauw, M. C.; Zwinselman, J. J.; Nibbering, N. M. M. *Org. Mass Spectrom.* **1982**, *17*. 274−276.
(20) Kulik, W.; Heerma, W. *Biomed. Mass Spectrom.* **1988**, *15*, 419−427.
(21) Posthumus, M. A.; Kistemaker, P. G.; Meuzelaar, H. L. C.; Ten Noever de Brauw, M. C. *Anal. Chem.* **1978**, *50*, 985−991.
(22) Schiller, C.; Kupka, D.; Hillenkamp, F. *Fresenius' Z. Anal. Chem.* **1981**, *308*, 304−308.
(23) Fan, T. P.; Hardin, E. D.; Vestal, M. L. *Anal. Chem.* **1984**, *56*, 1870−1876.
(24) Parker, C. D.; Hercules, D. M. *Anal. Chem.* **1985**. *57*, 698−704.
(25) Parker, C. D.; Hercules, D. M. *Anal. Chem.* **1986**, *58*, 25−30.
(26) Bouchonnet, S.; Denhez, J.-P.; Hoppilliard, Y.; Mauriac, C. *Anal. Chem.* **1992**, *64*, 743−754.
(27) Rogalewicz, F.; Hoppilliard, Y.; Ohanessian, G. *Int. J. Mass Spectrom.* **2000**, *195*/*196*, 565−590.

(28) Reid, G. E.; Simpson, R. J.; O'Hair, R. A. J. *J. Am. Soc. Mass Spectrom.* **2000**, *11*, 1047−1060.
(29) O'Hair, R. A. J.; Broughton, P. S.; Styles, M. L.; Frink, B. T.; Hadad, C. M. *J. Am. Soc. Mass Spectrom.* **2000**, *11*, 687−696.
(30) Uggerud, E. *Theor. Chem. Acc.* **1997**, *97*, 313−316.
(31) Rogalewicz, F.; Hoppilliard, Y. *Int. J. Mass Spectrom.* **2000**, *199*, 235−252.
(32) O'Hair, R. A. J.; Reid, G. E. *Eur. Mass Spectrom.* **1999**, *5*, 325−334.
(33) Becke, A. D. *Phys. Rev. A* **1988**, *38*, 3098−3100.
(34) Becke, A. D. *J. Chem. Phys.* **1993**, *98*, 5648−5652.
(35) Lee, C.; Yang, W.; Parr, R. G. *Phys. Rev. B* **1988**, *37*, 785−789.
(36) Hehre, W. J.; Ditchfield, R.; Pople, J. A. *J. Chem. Phys.* **1972**, *56*, 2257−2261.
(37) Chandrasekhar, J.; Andrade, J. G.; Schleyer, P. v. R. *J. Am. Chem. Soc.* **1981**, *103*, 5609−5612.
(38) Spitznagel, G. W.; Clark, T.; Chandrasekhar, J.; Schleyer, P. v. R. *J. Comput. Chem.* **1982**, *3*, 353−371.
(39) Hariharan, P. C.; Pople, J. A. *Chem. Phys. Lett.* **1972**, *16*, 217−219.
(40) Frisch, M. J.; Trucks, G. W.; Schlegel, H. B.; Scuseria, G. E.; Robb, M. A.; Cheeseman, J. R.; Zakrzewski, V. G.; Montgomery, J. A., Jr.; Stratmann, R. E.; Burant, J. C.; Dapprich, S.; Millam, J. M.; Daniels, A. D.; Kudin, K. N.; Strain, M. C.; Farkas, O.; Tomasi, J.; Barone, V.; Cossi, M.; Cammi, R.; Mennucci, B.; Pomelli, C.; Adamo, C.; Clifford, S.; Ochterski, J.; Petersson, G. A.; Ayala, P. Y.; Cui, Q.; Morokuma, K.; Malick, D. K.; Rabuck, A. D.; Raghavachari, K.; Foresman, J. B.; Cioslowski, J.; Ortiz, J. V.; Stefanov, B. B.; Liu, G.; Liashenko, A.; Piskorz, P.; Komaromi, I.; Gomperts, R.; Martin, R. L.; Fox, D. J.; Keith, T.; Al-Laham, M. A.; Peng, C. Y.; Nanayakkara, A.; Gonzalez, C.; Challacombe, M.; Gill, P. M. W.; Johnson, B. G.; Chen, W.; Wong, M. W.; Andres, J. L.; Head-Gordon, M.; Replogle, E. S.; Pople, J. A. *Gaussian 98*, revision A.11; Gaussian, Inc.: Pittsburgh, PA, 1998.
(41) Maksić, Z. B.; Kovačević, B. *Chem. Phys. Lett.* **1999**, *307*, 497−504.
(42) Dookeran, N. N.; Yalcin, T.; Harrison, A. G. *J. Mass Spectrom.* **1996**, *31*, 500−508.
(43) Shoeib, T.; Cunje, A.; Hopkinson, A. C.; Siu, K. W. M. *J. Am. Soc. Mass Spectrom.* **2002**, *13*, 408−416.
(44) Lioe, H.; O'Hair, R. A. J.; Reid, G. E. *J. Am. Soc. Mass Spectrom.* **2004**, *15*, 65−76.
(45) Rodriquez, C. F.; Cunje, A.; Shoeib, T.; Chu, I. K.; Hopkinson, A. C.; Siu, K. W. M. *J. Phys. Chem. A* **2000**, *104*, 5023−5028.
(46) Gassman, P. G.; Tidwell, T. T. *Acc. Chem. Res.* **1983**, *16*, 279−285.
(47) Grützmacher, H.-Fr.; Dommröse, A.-M. *Org. Mass Spectrom.* **1983**, *18*, 601−607.
(48) Dommröse, A.-M.; Grützmacher, H.-Fr. *Org. Mass Spectrom.* **1987**, *22*, 437−443.
(49) Wolf, R.; Grützmacher, H.-Fr. *Org. Mass Spectrom.* **1989**, *24*, 398−404.
(50) Wolf, R.; Grützmacher, H.-Fr. *J. Phys. Org. Chem.* **1990**, *3*, 301−308.
(51) Tkaczyk, M.; Harrison, A. G. *Int. J. Mass Spectrom. Ion Processes* **1991**, *109*, 295−304.
(52) Harrison, A. G.; Ichikawa, H. *Org. Mass Spectrom.* **1980**, *15*, 244−248.
(53) NIST Chemistry WebBook, http://webbook.nist.gov/chemistry.
(54) Beranova, S.; Cai, J.; Wesdemiotis, C. *J. Am. Chem. Soc.* **1995**, *117*, 9492−4501.
(55) Bouchoux, G.; Bourcier, S.; Hoppilliard, Y.; Mauriac, C. *Org. Mass Spectrom.* **1993**, *28*, 1064−1072.
(56) Shoeib, T.; El Aribi, H.; Rodriquez, C. F.; Hopkinson, A. C.; Siu, K. W. M. *J. Phys. Chem. A* **2001**, *105*, 710−719.
(57) El Aribi, H.; Shoeib, T.; Ling, Y.; Rodriquez, C. F.; Hopkinson, A. C.; Siu, K. W. M. *J. Phys. Chem. A* **2002**, *106*, 2908−2914.
(58) El Aribi, H.; Rodriquez, C. F.; Shoeib, T.; Ling, Y.; Hopkinson, A. C.; Siu, K. W. M. *J. Phys. Chem. A* **2002**, *106 (37)*, 8798−8805.
(59) El Aribi, H.; Rodriquez, C. F.; Almeida, D. R. P.; Ling, Y.; Mak, W. W.-N.; Hopkinson, A. C.; Siu, K. W. M. *J. Am. Chem. Soc.* **2003**, *125*, 9229−9236.
(60) Demmers, J. A. A.; Rijkers, D. T. S.; Haverkamp, J.; Killian, J. A.; Heck, A. J. R. *J. Am. Chem. Soc.* **2002**, *124*, 11191−11198.